

ORIGINAL RESEARCH ARTICLE

**SUPPLEMENTAL MATERIAL : Conformal normal curvature and detection of masked observations in multivariate null intercept measurement error models**

Reiko Aoki<sup>a</sup> , Juan P. Mamani Bustamante<sup>a</sup>, Cibele M. Russo<sup>a</sup> and Gilberto A. Paula<sup>b</sup>

<sup>a</sup> Instituto de Ciências Matemáticas e de Computação, Universidade de São Paulo, São Carlos - SP, Brazil; <sup>b</sup> Instituto de Matemática e Estatística, Universidade de São Paulo, São Paulo -SP, Brazil

**ARTICLE HISTORY**

Compiled April 25, 2023

**Contents**

<b>1</b>	<b>Multivariate QQ-Plot</b>	<b>2</b>
<b>2</b>	<b>Observed Information Matrix</b>	<b>2</b>
<b>3</b>	<b>Perturbation Schemes</b>	<b>3</b>
<b>4</b>	<b>Mouth Rinse Data</b>	<b>7</b>
4.1	Tables 1 and 2 . . . . .	7
4.2	Variance Perturbation Scheme . . . . .	7
4.3	Response Variable Perturbation Scheme . . . . .	9
4.4	Case Weight Perturbation Scheme . . . . .	10
<b>5</b>	<b>Hygroscopic Solid Dosage Data</b>	<b>14</b>
5.1	Variance Perturbation Scheme . . . . .	14
5.2	Case Weight Perturbation Scheme . . . . .	15

---

CONTACT Reiko Aoki. Email: reiko@icmc.usp.br

## 1. Multivariate QQ-Plot

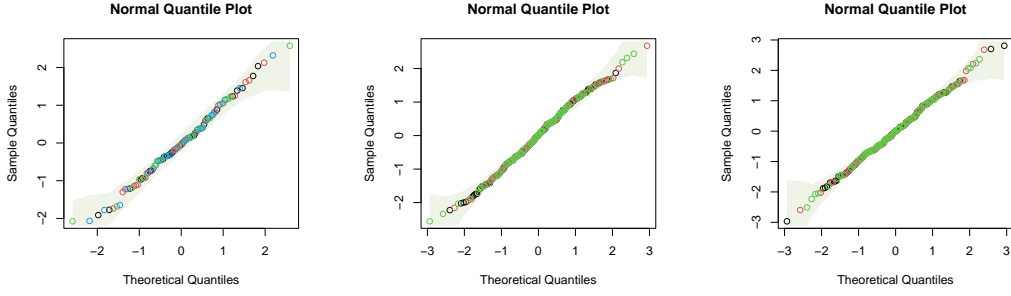


**Figure 1.** Multivariate QQ-Plot: Toothbrush Data (left hand panel) and Hygroscopic Solid Dosage Data (solid dosage A: middle panel and solid dosage B: right hand panel).

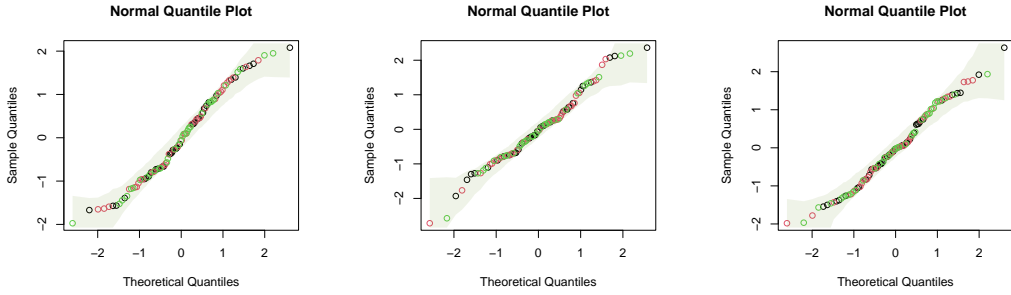


**Figure 2.** Multivariate QQ-Plot: Mouth Rinse Data. Control mouth rinse (left hand panel); experimental mouth rinse A (middle panel) and experimental mouth rinse B (right hand panel).

## 2. Observed Information Matrix

Considering the model defined in (3) and (4) the observed information matrix

$$-\ddot{L} = -\frac{\partial^2 \ell(\boldsymbol{\theta})}{\partial \boldsymbol{\theta} \partial \boldsymbol{\theta}^T},$$

were obtained in closed form expressions and the elements of the matrix are given by:

$$\frac{\partial^2 \ell(\boldsymbol{\theta})}{\partial \boldsymbol{\beta}_i \partial \boldsymbol{\beta}_i^T} = \sum_{j=1}^{n_i} \sigma_x^2 b_i^{-1} (\mathbf{D}^{-1}(\sigma_{e_i}^2) \mathbf{v}_{ij} \mathbf{v}_{ij}^T \mathbf{D}^{-1}(\sigma_{e_i}^2)) - 2\sigma_x^4 b_i^{-2} C_{ij} (\mathbf{D}^{-1}(\sigma_{e_i}^2) [\boldsymbol{\beta}_i \mathbf{v}_{ij}^T + \mathbf{v}_{ij} \boldsymbol{\beta}_i^T] \mathbf{D}^{-1}(\sigma_{e_i}^2)) + 2\sigma_x^4 b_i^{-2} (1 + 2\sigma_x^2 b_i^{-1} G_{ij}) \mathbf{D}^{-1}(\sigma_{e_i}^2) \boldsymbol{\beta}_i \boldsymbol{\beta}_i^T \mathbf{D}^{-1}(\sigma_{e_i}^2) - \{\mu^2 + \sigma_x^2 b_i^{-1} (1 + 2\mu C_{ij} + \sigma_x^2 b_i^{-1} G_{ij})\} \mathbf{D}^{-1}(\sigma_{e_i}^2);$$

$$\frac{\partial^2 \ell(\boldsymbol{\theta})}{\partial \boldsymbol{\beta}_i \partial \mu} = \sum_{j=1}^{n_i} -2b_i^{-2} C_{ij} \sigma_x^2 \mathbf{D}^{-1}(\sigma_{e_i}^2) \boldsymbol{\beta}_i + b_i^{-1} \mathbf{D}^{-1}(\sigma_{e_i}^2) \mathbf{v}_{ij};$$

$$\frac{\partial^2 \ell(\boldsymbol{\theta})}{\partial \boldsymbol{\beta}_i \partial \sigma_\delta^2} = \sum_{j=1}^{n_i} -\sigma_x^4 \sigma_\delta^{-4} b_i^{-2} \{1 - 2(x_{ij} - \mu) C_{ij} + 2\sigma_x^2 b_i^{-1} G_{ij}\} \mathbf{D}^{-1}(\sigma_{e_i}^2) \boldsymbol{\beta}_i \mathbf{D}^{-1}(\sigma_{e_i}^2) \boldsymbol{\beta}_i -$$

$$\begin{aligned}
& \sigma_x^2 \sigma_\delta^{-4} b_i^{-1} \{ (x_{i_j} - \mu) - \sigma_x^2 b_i^{-1} C_{i_j} \} \mathbf{D}^{-1}(\sigma_{e_i}^2) \mathbf{v}_{i_j}; \\
\frac{\partial^2 \ell(\boldsymbol{\theta})}{\partial \boldsymbol{\beta}_i \partial \sigma_x^2} &= \sum_{j=1}^{n_i} -b_i^{-2} \mathbf{D}^{-1}(\sigma_{e_i}^2) \boldsymbol{\beta}_i - 2b_i^{-3} \sigma_x^2 G_{i_j} \mathbf{D}^{-1}(\sigma_{e_i}^2) \boldsymbol{\beta}_i + b_i^{-2} C_{i_j} \mathbf{D}^{-1}(\sigma_{e_i}^2) \mathbf{v}_{i_j}; \\
\frac{\partial^2 \ell(\boldsymbol{\theta})}{\partial \boldsymbol{\beta}_i \partial \sigma_{e_i}^2} &= \sum_{j=1}^{n_i} \sigma_x^2 b_i^{-1} \{ -\mathbf{D}^{-1}(\sigma_{e_i}^2) \mathbf{v}_{i_j} \mathbf{d}_{i_j}^T \mathbf{D}^{-2}(\sigma_{e_i}^2) \mathbf{D}(\boldsymbol{\beta}_i) + \mathbf{D}^{-2}(\sigma_{e_i}^2) \mathbf{D}(\boldsymbol{\beta}_i) - \sigma_x^2 b_i^{-1} \\
& \quad \mathbf{D}^{-1}(\sigma_{e_i}^2) \boldsymbol{\beta}_i \boldsymbol{\beta}_i^T \mathbf{D}^{-2}(\sigma_{e_i}^2) \mathbf{D}(\boldsymbol{\beta}_i) \} - \mu \mathbf{D}^{-2}(\sigma_{e_i}^2) \mathbf{D}(\mathbf{d}_{i_j}) - \sigma_x^4 b_i^{-2} G_{i_j} \{ 2\sigma_x^2 b_i^{-1} \mathbf{D}^{-1}(\sigma_{e_i}^2) \\
& \quad \boldsymbol{\beta}_i \boldsymbol{\beta}_i^T \mathbf{D}^{-2}(\sigma_{e_i}^2) \mathbf{D}(\boldsymbol{\beta}_i) - \mathbf{D}^{-2}(\sigma_{e_i}^2) \mathbf{D}(\boldsymbol{\beta}_i) \} - \sigma_x^2 b_i^{-1} C_{i_j} \{ \mathbf{D}^{-2}(\sigma_{e_i}^2) \mathbf{D}(\mathbf{v}_{i_j}) - \sigma_x^2 b_i^{-1} \\
& \quad \mathbf{D}^{-1}(\sigma_{e_i}^2) [2\boldsymbol{\beta}_i \mathbf{d}_{i_j}^T + \mathbf{v}_{i_j} \boldsymbol{\beta}_i^T] \mathbf{D}^{-2}(\sigma_{e_i}^2) \mathbf{D}(\boldsymbol{\beta}_i) \}; \\
\frac{\partial^2 \ell(\mathbf{z}, \boldsymbol{\theta})}{\partial \mu \partial \mu} &= -\sum_{i=1}^p \sum_{j=1}^{n_i} \{ (1 - b_i^{-1}) \sigma_x^{-2} \}; \quad \frac{\partial^2 \ell(\boldsymbol{\theta})}{\partial \mu \partial \sigma_x^2} = -\sum_{i=1}^p \sum_{j=1}^{n_i} (b_i^{-1} - b_i^{-2}) \sigma_x^{-2} C_{i_j}; \\
\frac{\partial^2 \ell(\boldsymbol{\theta})}{\partial \mu \partial \sigma_\delta^2} &= -\sum_{i=1}^p \sum_{j=1}^{n_i} b_i^{-1} \sigma_\delta^{-4} \{ (x_{i_j} - \mu) - \sigma_x^2 b_i^{-1} C_{i_j} \}; \\
\frac{\partial^2 \ell(\boldsymbol{\theta})}{\partial \mu \partial \sigma_{e_i}^2} &= \sum_{j=1}^{n_i} b_i^{-2} \sigma_x^2 C_{i_j} \boldsymbol{\beta}_i^T \mathbf{D}^{-2}(\sigma_{e_i}^2) \mathbf{D}(\boldsymbol{\beta}_i) - b_i^{-1} \mathbf{d}_{i_j}^T \mathbf{D}^{-2}(\sigma_{e_i}^2) \mathbf{D}(\boldsymbol{\beta}_i); \\
\frac{\partial^2 \ell(\boldsymbol{\theta})}{\partial \sigma_x^2 \partial \sigma_\delta^2} &= -\frac{1}{2} \sum_{i=1}^p \sum_{j=1}^{n_i} \{ -\sigma_\delta^{-4} + (2 - \sigma_x^2 \sigma_\delta^{-2} b_i^{-1}) \sigma_\delta^{-6} \sigma_x^2 b_i^{-1} - 4\sigma_x^2 \sigma_\delta^{-6} b_i^{-1} (1 - \sigma_x^2 \sigma_\delta^{-2} b_i^{-1}) \\
& \quad (x_{i_j} - \mu) C_{i_j} + 2\sigma_x^4 \sigma_\delta^{-6} b_i^{-2} (1 - \sigma_x^2 \sigma_\delta^{-2} b_i^{-1}) G_{i_j} + 2\sigma_\delta^{-6} (1 - \sigma_x^2 \sigma_\delta^{-2} b_i^{-1}) (x_{i_j} - \mu)^2 \}; \\
\frac{\partial^2 \ell(\boldsymbol{\theta})}{\partial \sigma_x^2 \partial \sigma_x^2} &= -\frac{1}{2} \sum_{i=1}^p \sum_{j=1}^{n_i} \{ -\sigma_\delta^{-4} b_i^{-2} - 2b_i^{-3} \sigma_x^2 \sigma_\delta^{-4} G_{i_j} + 2b_i^{-2} \sigma_\delta^{-4} (x_{i_j} - \mu) C_{i_j} \}; \\
\frac{\partial^2 \ell(\boldsymbol{\theta})}{\partial \sigma_x^2 \partial \sigma_{e_i}^2} &= -\frac{1}{2} \sum_{j=1}^{n_i} \{ b_i^{-2} \sigma_\delta^{-4} \{ \sigma_x^4 [2(x_{i_j} - \mu) C_{i_j} - 2\sigma_x^2 G_{i_j} b_i^{-1} - 1] \boldsymbol{\beta}_i^T \mathbf{D}^{-2}(\sigma_{e_i}^2) \mathbf{D}(\boldsymbol{\beta}_i) \} - \\
& \quad b_i^{-1} \sigma_\delta^{-4} (2\sigma_x^2 (x_{i_j} - \mu - \sigma_x^2 b_i^{-1} C_{i_j}) \mathbf{d}_{i_j}^T \mathbf{D}^{-2}(\sigma_{e_i}^2) \mathbf{D}(\boldsymbol{\beta}_i)) \}; \\
\frac{\partial^2 \ell(\boldsymbol{\theta})}{\partial \sigma_x^2 \partial \sigma_x^2} &= -\frac{1}{2} \sum_{i=1}^p \sum_{j=1}^{n_i} \{ -\sigma_x^{-4} [1 - b_i^{-1} (2 - b_i^{-1})] + 2\sigma_x^{-2} b_i^{-2} (1 - b_i^{-1}) G_{i_j} \}; \\
\frac{\partial^2 \ell(\boldsymbol{\theta})}{\partial \sigma_x^2 \partial \sigma_{e_i}^2} &= \frac{1}{2} \sum_{j=1}^{n_i} \{ b_i^{-2} (1 + 2b_i^{-1} \sigma_x^2 G_{i_j}) \boldsymbol{\beta}_i^T \mathbf{D}^{-2}(\sigma_{e_i}^2) \mathbf{D}(\boldsymbol{\beta}_i) - 2b_i^{-2} C_{i_j} \mathbf{d}_{i_j}^T \mathbf{D}^{-2}(\sigma_{e_i}^2) \\
& \quad \mathbf{D}(\boldsymbol{\beta}_i) \}; \\
\frac{\partial^2 \ell(\boldsymbol{\theta})}{\partial \sigma_{e_i}^2 \partial \sigma_{e_i}^2} &= \frac{1}{2} \sum_{j=1}^{n_i} \{ -2\mathbf{D}(\mathbf{d}_{i_j}) \mathbf{D}^{-3}(\sigma_{e_i}^2) \mathbf{D}(\mathbf{d}_{i_j}) + 2\sigma_x^2 b_i^{-1} \mathbf{D}(\boldsymbol{\beta}_i) \mathbf{D}^{-2}(\sigma_{e_i}^2) \mathbf{d}_{i_j} \mathbf{d}_{i_j}^T \\
& \quad \mathbf{D}^{-2}(\sigma_{e_i}^2) \mathbf{D}(\boldsymbol{\beta}_i) - \sigma_x^2 b_i^{-1} [2\mathbf{D}(\boldsymbol{\beta}_i) \mathbf{D}^{-3}(\sigma_{e_i}^2) \mathbf{D}(\boldsymbol{\beta}_i) - \sigma_x^2 b_i^{-1} \mathbf{D}(\boldsymbol{\beta}_i) \mathbf{D}^{-2}(\sigma_{e_i}^2) \boldsymbol{\beta}_i \boldsymbol{\beta}_i^T \\
& \quad \mathbf{D}^{-2}(\sigma_{e_i}^2) \mathbf{D}(\boldsymbol{\beta}_i)] - 2\sigma_x^4 b_i^{-2} G_{i_j} [\mathbf{D}(\boldsymbol{\beta}_i) \mathbf{D}^{-3}(\sigma_{e_i}^2) \mathbf{D}(\boldsymbol{\beta}_i) - \sigma_x^2 b_i^{-1} \mathbf{D}(\boldsymbol{\beta}_i) \mathbf{D}^{-2}(\sigma_{e_i}^2) \boldsymbol{\beta}_i \boldsymbol{\beta}_i^T \\
& \quad \mathbf{D}^{-2}(\sigma_{e_i}^2) \mathbf{D}(\boldsymbol{\beta}_i)] + 4\sigma_x^2 b_i^{-1} C_{i_j} (\mathbf{D}(\boldsymbol{\beta}_i) \mathbf{D}^{-3}(\sigma_{e_i}^2) \mathbf{D}(\mathbf{d}_{i_j}) - \frac{1}{2} \sigma_x^2 b_i^{-1} \mathbf{D}(\boldsymbol{\beta}_i) \mathbf{D}^{-2}(\sigma_{e_i}^2) \\
& \quad (\boldsymbol{\beta}_i \mathbf{d}_{i_j}^T + \mathbf{d}_{i_j} \boldsymbol{\beta}_i^T) \mathbf{D}^{-2}(\sigma_{e_i}^2) \mathbf{D}(\boldsymbol{\beta}_i)) + \mathbf{D}^{-2}(\sigma_{e_i}^2) \}; \\
\end{aligned}$$

with  $C_{i_j}$ ,  $v_{i_j}$  and  $G_{i_j}$  as defined in Section 3 of the manuscript.

### 3. Perturbation Schemes

Let

$$\Delta_{((4p+3) \times N)} = \frac{\partial^2 \ell(\boldsymbol{\theta} | \boldsymbol{\omega})}{\partial \boldsymbol{\theta} \partial \boldsymbol{\omega}^T} \Big|_{\boldsymbol{\theta} = \hat{\boldsymbol{\theta}}, \boldsymbol{\omega} = \boldsymbol{\omega}_0} = (\Delta_{\theta_1}, \dots, \Delta_{\theta_{p_{n_p}}}) \Big|_{\boldsymbol{\theta} = \hat{\boldsymbol{\theta}}, \boldsymbol{\omega} = \boldsymbol{\omega}_0},$$

where  $\Delta\theta_{i_j} = (\Delta_{\beta_1 i_j}^T, \dots, \Delta_{\beta_p i_j}^T, \Delta_{\mu i_j}, \Delta_{\sigma_x^2 i_j}, \Delta_{\sigma_\delta^2 i_j}, \Delta_{\sigma_{e_1}^2 i_j}, \dots, \Delta_{\sigma_{e_p}^2 i_j}^T)_{((4p+3)\times 1)}^T$ ,  $i = 1, \dots, p$ ,  $j = 1, \dots, n_i$ , and  $N = \sum_{i=1}^p n_i$ .

After algebraic manipulations, the elements of the matrix  $\Delta$  for each perturbation scheme were obtained and are given as follows:

- Explanatory variable perturbation scheme

In this case, the observed value of the perturbed covariate is given by

$$x_{i_j\omega} = x_{i_j} + S_x \omega_{i_j},$$

$i = 1, \dots, p$ ,  $j = 1, \dots, n_i$ , where  $S_x$  is some scale factor, so that the perturbed log likelihood function may be written as

$$\ell(\boldsymbol{\theta} \mid \boldsymbol{\omega}) = -\frac{3N}{2} \log(2\pi) - \frac{1}{2} \sum_{i=1}^p n_i \log |\mathbf{V}_i| - \frac{1}{2} \sum_{i=1}^p \sum_{j=1}^{n_i} (\mathbf{z}_{i_j}^* - \mathbf{m}_i)^T \mathbf{V}_i^{-1} (\mathbf{z}_{i_j}^* - \mathbf{m}_i),$$

with  $\mathbf{z}_{i_j}^* = (x_{i_j} + S_x \omega_{i_j}, y_{1i_j}, y_{2i_j})^T$  and the no perturbation vector  $\boldsymbol{\omega}_0 = \mathbf{0}_N = (0, \dots, 0)^T$ . The elements of the matrix  $\Delta$  are given by

$$\begin{aligned} \Delta_{\beta_i i_j} &= \sigma_x^2 \sigma_\delta^{-2} b_i^{-1} S_x \{-2\sigma_x^2 b_i^{-1} C_{i_j} \mathbf{D}^{-1}(\sigma_{e_i}^2) \boldsymbol{\beta}_i + \mathbf{D}^{-1}(\sigma_{e_i}^2) \mathbf{v}_{i_j}\}; \\ \Delta_{\mu i_j} &= S_x \sigma_\delta^{-2} b_i^{-1}; \\ \Delta_{\sigma_\delta^2 i_j} &= \sigma_\delta^{-4} S_x (1 - \sigma_\delta^{-2} \sigma_x^2 b_i^{-1}) [(x_{i_j} - \mu) - \sigma_x^2 C_{i_j} b_i^{-1}]; \\ \Delta_{\sigma_x^2 i_j} &= \sigma_\delta^{-2} b_i^{-2} S_x C_{i_j}; \\ \Delta_{\sigma_{e_i}^2 i_j} &= S_x \sigma_x^2 b_i^{-1} \sigma_\delta^{-2} \{\sigma_x^2 b_i^{-1} C_{i_j} \mathbf{D}(\boldsymbol{\beta}_i) \mathbf{D}^{-2}(\sigma_{e_i}^2) \boldsymbol{\beta}_i - \mathbf{D}(\boldsymbol{\beta}_i) \mathbf{D}^{-2}(\sigma_{e_i}^2) \mathbf{d}_{i_j}\}. \end{aligned}$$

- Case weight perturbation scheme

The log likelihood function of the perturbed model is given by

$$\ell(\boldsymbol{\theta} \mid \boldsymbol{\omega}) = \sum_{i=1}^p \sum_{j=1}^{n_i} \omega_{i_j} \log f(\mathbf{z}_{i_j}, \boldsymbol{\theta})$$

$$= -\frac{3}{2} \log(2\pi) \sum_{i=1}^p \sum_{j=1}^{n_i} \omega_{i_j} - \frac{1}{2} \sum_{j=1}^{n_i} \omega_{i_j} - \frac{1}{2} \sum_{i=1}^p \sum_{j=1}^{n_i} \omega_{i_j} (\mathbf{z}_{i_j} - \mathbf{m}_i)^T \mathbf{V}_i^{-1} (\mathbf{z}_{i_j} - \mathbf{m}_i),$$

with the no perturbation vector  $\boldsymbol{\omega}_0 = \mathbf{1}_N = (1, \dots, 1)^T$ . Then, the elements of the matrix  $\Delta$  are given by

$$\begin{aligned} \Delta_{\beta_i i_j} &= (\mu + \sigma_x^2 b_i^{-1} C_{i_j}) \mathbf{D}^{-1}(\sigma_{e_i}^2) \mathbf{d}_{i_j} - \sigma_x^2 b_i^{-1} (1 + \sigma_x^2 b_i^{-1} G_{i_j} + \mu C_{i_j}) \mathbf{D}^{-1}(\sigma_{e_i}^2) \boldsymbol{\beta}_i; \\ \Delta_{\mu i_j} &= b_i^{-1} C_{i_j}; \\ \Delta_{\sigma_\delta^2 i_j} &= -\frac{1}{2} \{\sigma_\delta^{-2} [1 - \sigma_\delta^{-2} (\sigma_x^2 b_i^{-1} + (x_{i_j} - \mu)^2)] + \sigma_x^2 \sigma_\delta^{-4} b_i^{-1} [2(x_{i_j} - \mu) C_{i_j} - \sigma_x^2 b_i^{-1} G_{i_j}]\}; \\ \Delta_{\sigma_x^2 i_j} &= -\frac{1}{2} \{\sigma_x^{-2} (1 - b_i^{-1}) - b_i^{-2} G_{i_j}\}; \end{aligned}$$

$$\begin{aligned}\Delta_{\sigma_{e_i}^2 i_j} &= \frac{1}{2} \mathbf{D}(D_{ij}) \mathbf{D}^{-2}(\boldsymbol{\sigma}_{e_i}^2) \mathbf{d}_{i_j} - \sigma_x^2 b_i^{-1} C_{i_j} \mathbf{D}(\boldsymbol{\beta}_i) \mathbf{D}^{-2}(\boldsymbol{\sigma}_{e_i}^2) \mathbf{d}_{i_j} + \frac{1}{2} \sigma_x^2 b_i^{-1} \{ \sigma_x^2 b_i^{-1} \\ &G_{i_j} + 1 \} \mathbf{D}(\boldsymbol{\beta}_i) \mathbf{D}^{-2}(\boldsymbol{\sigma}_{e_i}^2) \boldsymbol{\beta}_i - \frac{1}{2} \mathbf{D}^{-1}(\boldsymbol{\sigma}_{e_i}^2) \mathbf{1}_2;\end{aligned}$$

$$i = 1, \dots, p, j = 1, \dots, n_i.$$

- Variance perturbation scheme

In this perturbation, we perturb the measurement error variances, so that

$$\sigma_{\delta\omega}^2 = \frac{\sigma_\delta^2}{\omega_{i_j}}, \sigma_{e_1\omega}^2 = \frac{\sigma_{e_1}^2}{\omega_{i_j}} \text{ and } \sigma_{e_2\omega}^2 = \frac{\sigma_{e_2}^2}{\omega_{i_j}},$$

$i = 1, \dots, p, j = 1, \dots, n_i$ . Thus, the log likelihood function of the perturbed model is given by

$$\begin{aligned}\ell(\boldsymbol{\theta} | \boldsymbol{\omega}) &= -\frac{3N}{2} \log(2\pi) - \frac{1}{2} \sum_{i=1}^p \sum_{j=1}^{n_i} \log |\mathbf{V}_{i_j}^{**}| - \\ &\frac{1}{2} \sum_{i=1}^p \sum_{j=1}^{n_i} (\mathbf{z}_{i_j} - \mathbf{m}_i)^T (\mathbf{V}_{i_j}^{**})^{-1} (\mathbf{z}_{i_j} - \mathbf{m}_i),\end{aligned}$$

with

$$\mathbf{V}_{i_j}^{**} = \begin{bmatrix} \sigma_x^2 + \frac{\sigma_\delta^2}{\omega_{i_j}} & \beta_{1i} \sigma_x^2 & \beta_{2i} \sigma_x^2 \\ \beta_{1i} \sigma_x^2 & \beta_{1i}^2 \sigma_x^2 + \frac{\sigma_{e_1i}^2}{\omega_{i_j}} & \beta_{1i} \beta_{2i} \sigma_x^2 \\ \beta_{2i} \sigma_x^2 & \beta_{1i} \beta_{2i} \sigma_x^2 & \beta_{2i}^2 \sigma_x^2 + \frac{\sigma_{e_2i}^2}{\omega_{i_j}} \end{bmatrix} \quad (1)$$

and the no perturbation vector  $\boldsymbol{\omega}_0 = \mathbf{1}_N = (1, \dots, 1)^T$ . The elements of the matrix  $\Delta$ , in this case, are given by

$$\begin{aligned}\Delta_{\beta_i i_j} &= -\sigma_x^2 b_i^{-2} \mathbf{D}^{-1}(\boldsymbol{\sigma}_{e_i}^2) \boldsymbol{\beta}_i + \mu \mathbf{D}^{-1}(\boldsymbol{\sigma}_{e_i}^2) \mathbf{d}_{i_j} + \sigma_x^2 \left[ -\sigma_x^2 b_i^{-3} (2 + b_i) C_{i_j}^2 \mathbf{D}^{-1}(\boldsymbol{\sigma}_{e_i}^2) \right. \\ &\left. \boldsymbol{\beta}_i + b_i^{-2} (1 + b_i) C_{i_j} \mathbf{D}^{-1}(\boldsymbol{\sigma}_{e_i}^2) (\mathbf{y}_{i_j} - 2\boldsymbol{\beta}_i \mu) \right];\end{aligned}$$

$$\Delta_{\mu i_j} = b_i^{-2} C_{i_j};$$

$$\begin{aligned}\Delta_{\sigma_\delta^2 i_j} &= -\frac{1}{2} \left\{ -\sigma_\delta^{-4} \sigma_x^2 b_i^{-2} - \sigma_\delta^{-4} \left[ (x_{i_j} - \mu)^2 + \sigma_x^2 b_i^{-3} C_{i_j} (\sigma_x^2 C_{i_j} (2 + b_i) - 2b_i \right. \right. \\ &\left. \left. (b_i + 1)(x_{i_j} - \mu)) \right] \right\};\end{aligned}$$

$$\Delta_{\sigma_x^2 i_j} = -\frac{b_i^{-3}}{2} \left\{ \sigma_x^{-2} b_i (b_i - 1) - 2C_{i_j}^2 \right\};$$

$$\begin{aligned}\Delta_{\sigma_{e_i}^2 i_j} &= -\frac{1}{2} \left\{ -\sigma_x^2 b_i^{-2} \mathbf{D}(\boldsymbol{\beta}_i) \mathbf{D}^{-2}(\boldsymbol{\sigma}_{e_i}^2) \boldsymbol{\beta}_i - \mathbf{D}(\mathbf{d}_{i_j}) \mathbf{D}^{-2}(\boldsymbol{\sigma}_{e_i}^2) \mathbf{d}_{i_j} - \sigma_x^2 b_i^{-3} C_{i_j} \left[ \sigma_x^2 \right. \right. \\ &\left. \left. (b_i + 2) C_{i_j} \mathbf{D}(\boldsymbol{\beta}_i) \mathbf{D}^{-2}(\boldsymbol{\sigma}_{e_i}^2) \boldsymbol{\beta}_i - 2b_i (b_i + 1) \mathbf{D}(\boldsymbol{\beta}_i) \mathbf{D}^{-2}(\boldsymbol{\sigma}_{e_i}^2) \mathbf{d}_{i_j} \right] \right\};.\end{aligned}$$

$i = 1, \dots, p, j = 1, \dots, n_i$ .

- Response variable perturbation scheme

Consider the following perturbation in the response variables

$$\begin{cases} y_{1i_j\omega} = y_{1i_j} + S_{y_{1i}}\omega_{i_j} \\ y_{2i_j\omega} = y_{2i_j} + S_{y_{2i}}\omega_{i_j}, i = 1, \dots, p, j = 1, \dots, n_i, \end{cases}$$

where  $S_{y_{1i}}$  and  $S_{y_{2i}}$  are scale factors. The perturbed log likelihood function in this case is given by

$$\ell(\boldsymbol{\theta} \mid \boldsymbol{\omega}) = -\frac{3N}{2} \log(2\pi) - \frac{1}{2} \sum_{i=1}^p n_i \log |\mathbf{V}_i| - \frac{1}{2} \sum_{i=1}^p \sum_{j=1}^{n_i} (\mathbf{z}_{i_j}^{**} - \mathbf{m}_i)^T \mathbf{V}_i^{-1} (\mathbf{z}_{i_j}^{**} - \mathbf{m}_i),$$

with  $\mathbf{z}_{i_j}^{**} = (x_{i_j}, y_{1i_j} + S_{y_{1i}}\omega_{i_j}, y_{2i_j} + S_{y_{2i}}\omega_{i_j})^T$  and the no perturbation vector  $\boldsymbol{\omega}_0 = \mathbf{0}_N = (0, \dots, 0)^T$ . The elements of the matrix  $\Delta$  can be written as

$$\begin{aligned} \Delta_{\beta_i i_j} &= \sigma_x^2 b_i^{-1} (\boldsymbol{\beta}_i^T \mathbf{D}^{-1}(\boldsymbol{\sigma}_{e_i}^2) \mathbf{S}_{y_i}) (\mathbf{D}^{-1}(\boldsymbol{\sigma}_{e_i}^2) (\mathbf{y}_{i_j} - 2\boldsymbol{\beta}_i \mu) - 2b_i^{-1} \sigma_x^2 C_{i_j} \mathbf{D}^{-1}(\boldsymbol{\sigma}_{e_i}^2) \boldsymbol{\beta}_i) \\ &\quad + (\sigma_x^2 b_i^{-1} C_{i_j} + \mu) \mathbf{D}^{-1}(\boldsymbol{\sigma}_{e_i}^2) \mathbf{S}_{y_i}; \\ \Delta_{\mu i_j} &= b_i^{-1} (\boldsymbol{\beta}_i^T \mathbf{D}^{-1}(\boldsymbol{\sigma}_{e_i}^2) \mathbf{S}_{y_i}); \\ \Delta_{\sigma_{\delta}^2 i_j} &= \sigma_x^2 \sigma_{\delta}^{-4} b_i^{-1} (\sigma_x^2 b_i^{-1} C_{i_j} - (x_{i_j} - \mu)) (\boldsymbol{\beta}_i^T \mathbf{D}^{-1}(\boldsymbol{\sigma}_{e_i}^2) \mathbf{S}_{y_i}); \\ \Delta_{\sigma_x^2 i_j} &= b_i^{-2} C_{i_j} (\boldsymbol{\beta}_i^T \mathbf{D}^{-1}(\boldsymbol{\sigma}_{e_i}^2) \mathbf{S}_{y_i}); \end{aligned}$$

$$\begin{aligned} \Delta_{\sigma_{e_i}^2 i_j} &= \mathbf{D}(\mathbf{S}_{y_i}) \mathbf{D}^{-2}(\boldsymbol{\sigma}_{e_i}^2) \mathbf{d}_{i_j} - \sigma_x^2 b_i^{-1} C_{i_j} \mathbf{D}(\boldsymbol{\beta}_i) \mathbf{D}^{-2}(\boldsymbol{\sigma}_{e_i}^2) \mathbf{S}_{y_i} \sigma_x^2 b_i^{-1} (\boldsymbol{\beta}_i^T \mathbf{D}^{-1}(\boldsymbol{\sigma}_{e_i}^2) \\ &\quad \mathbf{S}_{y_i}) (\sigma_x^2 b_i^{-1} C_{i_j} \mathbf{D}(\boldsymbol{\beta}_i) \mathbf{D}^{-2}(\boldsymbol{\sigma}_{e_i}^2) \boldsymbol{\beta}_i - \mathbf{D}(\boldsymbol{\beta}_i) \mathbf{D}^{-2}(\boldsymbol{\sigma}_{e_i}^2) \mathbf{d}_{i_j}); \end{aligned}$$

with  $\boldsymbol{\beta}_i, \boldsymbol{\sigma}_{e_i}^2, \mathbf{a}_i, \mathbf{A}_i, \mathbf{B}_i$ , and  $b_i, i = 1, \dots, p$ , as defined in (??) and (??), and  $C_{i_j} = \sigma_{\delta}^{-2} (x_{i_j} - \mu) + ((\mathbf{y}_{i_j} - \boldsymbol{\beta}_i \mu)^T \mathbf{D}^{-1}(\boldsymbol{\sigma}_{e_i}^2) \boldsymbol{\beta}_i) = [\mathbf{a}_i^T \mathbf{A}_i^{-1} (\mathbf{z}_{i_j} - \mathbf{m}_i)]; \mathbf{d}_{i_j} = (\mathbf{y}_{i_j} - \boldsymbol{\beta}_i \mu); \mathbf{v}_{i_j} = (\mathbf{y}_{i_j} - 2\boldsymbol{\beta}_i \mu)$  and  $G_{i_j} = \sigma_{\delta}^{-4} (x_{i_j} - \mu)^2 + 2\sigma_{\delta}^{-2} (x_{i_j} - \mu) (\mathbf{y}_{i_j} - \boldsymbol{\beta}_i \mu)^T \mathbf{D}^{-1}(\boldsymbol{\sigma}_{e_i}^2) \boldsymbol{\beta}_i + (\mathbf{y}_{i_j} - \boldsymbol{\beta}_i \mu)^T \mathbf{D}^{-1}(\boldsymbol{\sigma}_{e_i}^2) \boldsymbol{\beta}_i \boldsymbol{\beta}_i^T \mathbf{D}^{-1}(\boldsymbol{\sigma}_{e_i}^2) (\mathbf{y}_{i_j} - \boldsymbol{\beta}_i \mu) = [(\mathbf{z}_{i_j} - \mathbf{m}_i)^T \mathbf{B}_i (\mathbf{z}_{i_j} - \mathbf{m}_i)]$ .

For the model defined in (1) and (2) of the manuscript, these matrices can be found in Aoki [3].

## 4. Mouth Rinse Data

### 4.1. Tables 1 and 2

**Table 1.** P-values from the hypothesis testing for assessing the long term homogeneity, after six months from the baseline, of the experimental mouth rinse A and B with all the observations and by dropping subsets of observations ( $H_0 : \beta_{2_2} = \beta_{2_3}$ ).

complete data	without the observations						
	42	52	67	80	(22,42)	(42,67)	(39,40,43)
p-value	0.154	0.163	0.122	0.139	0.154	0.194	0.017

**Table 2.** P-values from the hypothesis testing for assessing the long term homogeneity, after three months from the baseline, of the control mouth rinse and the experimental mouth rinse A with all the observations and by dropping subsets of observations ( $H_0 : \beta_{1_1} = \beta_{1_2}$ ).

complete data	without the observations			
	(39,40,43)	(39,40,43,42)	(39,40,43,52)	
p-value	0.002	0.015	0.007	0.082

### 4.2. Variance Perturbation Scheme

In this subsection, we consider the variance perturbation scheme with the contribution of eigenvector associated with the largest eigenvalue.

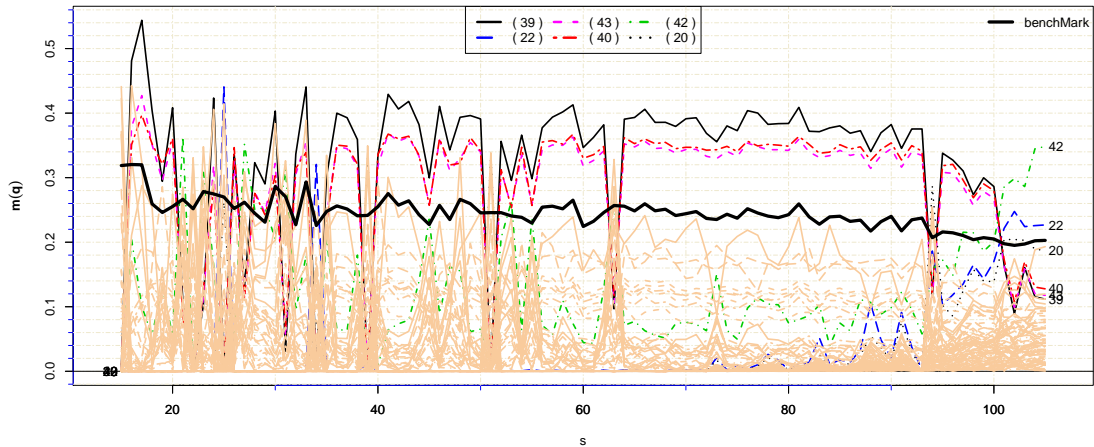


**Figure 3.** Mouth rinse data: CNCFS forward plot for variance perturbation scheme. Contribution of the eigenvector associated with the largest eigenvalue.

Figure 3 shows that although observations 42 and 22 are above the benchmark in the final iteration (see also Figure 4, left hand panel) observations 39, 40 and 43 are mostly above the benchmark for almost the entire CNCFS evolution and they are masked in the final steps. On the other hand, observations 22 and 42 pop up in the

final steps. Furthermore, observation 20 pops up in the final steps and it is masked right after.

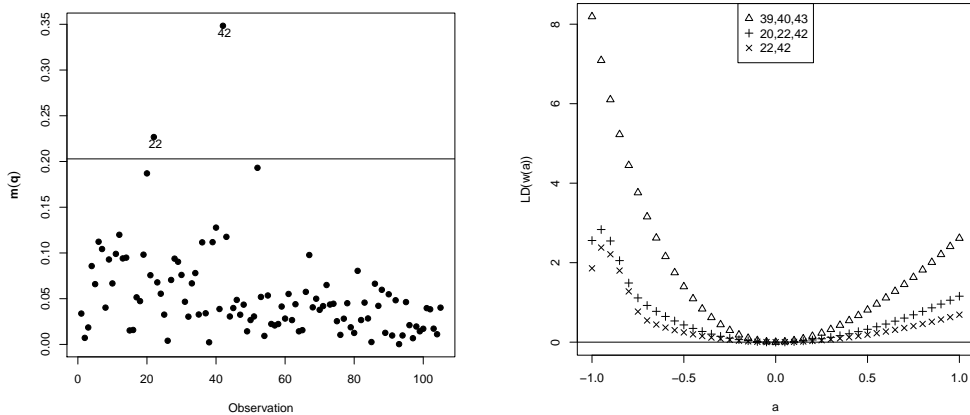


**Figure 4.** Mouth rinse data: Aggregate contribution of eigenvector associated with the largest eigenvalue, variance perturbation scheme. Index plot of  $m(q)$  (left hand panel) and plot of  $LD(\omega(a))$  versus  $a$  with  $\omega(a) = \omega_o + al$  (right hand panel).

To analyze the influence of these observations in the likelihood displacement, the right hand panel of Figure 4 shows the plot of  $LD(\omega_0 + al)$  versus  $a \in [-1, 1]$  along the directions  $l = l_k$ , with  $k = (22, 42)$ ,  $(20, 22, 42)$  and  $(39, 40, 43)$ , which are, respectively, the observations that are above the benchmark in the last iteration, observations that pop up in the final steps and observations that were masked in the final iterations. Clearly if we perturb in the direction of the group of observations  $(39, 40, 43)$ , which were masked in the final steps, the likelihood displacement increases more than if we perturb in the direction of the group of observations  $(22, 42)$ , which are above the benchmark in the final step, so these observations are less influential together than the group of observations  $(39, 40, 43)$ . In addition it was considered the direction  $(20, 22, 42)$  to see the influence of the observation 20 that also popped up in the final steps, but was masked. In this case, if we perturb in the direction of the three observations  $(20, 22, 42)$  that popped up in the final steps, there is a slight increase in the likelihood displacement than if we perturb in the direction of  $(22, 42)$ .

Considering the hypotheses of interest, Table 1 shows that the removal of observation 42 change the conclusion of the hypothesis testing at significance level 10%, i.e with the removal of the observation 42 the hypothesis that the dental plaque index reduction rate after 6 months using the experimental mouth rinse A and B are the same is no longer rejected. The same happens if we drop the group of observations  $(22,42)$  together. However, if we drop the observations 20, 22, 39, 40 or 43 individually, they do not affect the inferential result of this hypothesis testing (not shown here). On the other hand, if we drop observation 42 (global influence) from the data set and obtain the new maximum likelihood estimates of the parameters (not shown here), the relative change in the estimated values are small.

Moreover, if we drop the group of observations  $(39, 40, 43)$ , which was masked in the final steps, they change the result of this hypothesis testing at significance level 5%.

Table 2 considers the hypothesis that the dental plaque index reduction of the adults who used the control mouth rinse and the experimental mouth rinse A after



three months are the same. This hypothesis is rejected with complete data. However, if we remove the group of observations (39,40,43) it is no longer rejected at significance level of 5 %. Also, the removal of the observations 22, 42, 39, 40 or 43 individually or the removal of group of observations (22,42), which appears above the bench mark in the final step, do not change the inferential results (not shown here).

### 4.3. Response Variable Perturbation Scheme

Next, we consider the response variable perturbation scheme. Figure 5 gives the forward plot of CNCFS considering the contribution of the eigenvector associated with the largest eigenvalue.

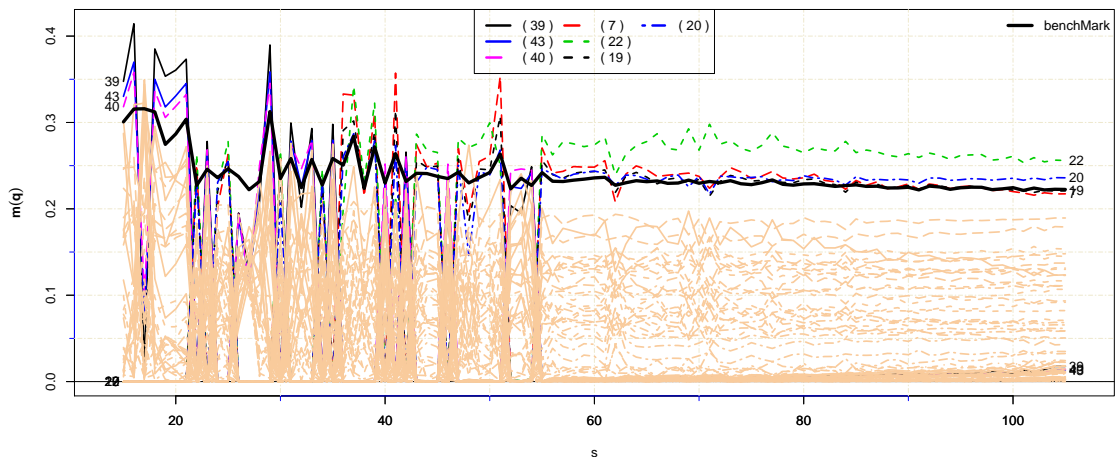


**Figure 5.** Mouth rinse data: CNCFS forward plot for response variable perturbation scheme. Contribution of the eigenvector associated with the largest eigenvalue. Index plot of  $m(q)$ .

Though observations 20 and 22 are above the benchmark in the final step of the evolution of the forward plot (see also Figure 6, left hand panel), observations 7 and 19 are very close to the benchmark in the final step.

Analyzing these observations, we see that they are detached from the rest of observations from iteration  $s = 55$  to the end of CNCFS evolution. Also, observation 7 are mostly above the benchmark from iteration  $s = 36$  to iteration  $s = 85$ , but it is masked in the final steps. Subject 7 had the greatest plaque index reduction from the beginning of the study to the end of the treatment among adults who took the control treatment. In addition, individual 7 had the least plaque index after 6 months and the second least plaque index in the beginning of the study among subjects who used the control mouth rinse.

The right hand panel of Figure 6 shows the plot of  $LD(\omega_0 + a\mathbf{l})$  versus  $a \in [-1, 1]$  along the directions  $\mathbf{l} = \mathbf{l}_k$ , with  $k = 7, 19, 20$  and 22. It shows that observation 22 gives the largest change in the likelihood displacement followed by the observation 7, though the influence of these observations (7, 19, 20, 22) are close.

Also, observations 39, 40 and 43 appears above the benchmark in the beginning of CNCFS evolution. These observations also appeared in the variance perturbation scheme and they were above the benchmark in almost the entire CNCFS evolution (see Figure 3). This group of observations was already analyzed and the conclusion

was that they are jointly influential as it leads to inferential changes.

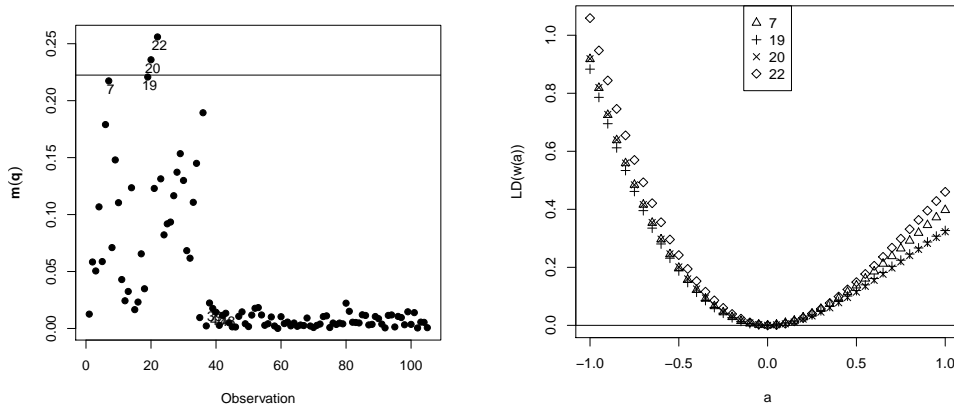


**Figure 6.** Mouth rinse data: Contribution of the eigenvector associated with the largest eigenvalue, response variable perturbation scheme. Index plot of  $m(q)$  (left hand panel) and plot of  $LD(\omega(a))$  versus  $a$  with  $\omega(a) = \omega_o + al$  (right hand panel).

Moreover, Figure 6 (left hand panel) shows the index plot of  $m(q)$  corresponding to the last iteration of Figure 5. It can be seen that small local changes in the response variable corresponding to the control mouth rinse treatment have a larger effect on the parameter estimates.

#### 4.4. Case Weight Perturbation Scheme

Finally, Figure 7 shows the CNCFS forward plots for case weight perturbation scheme.

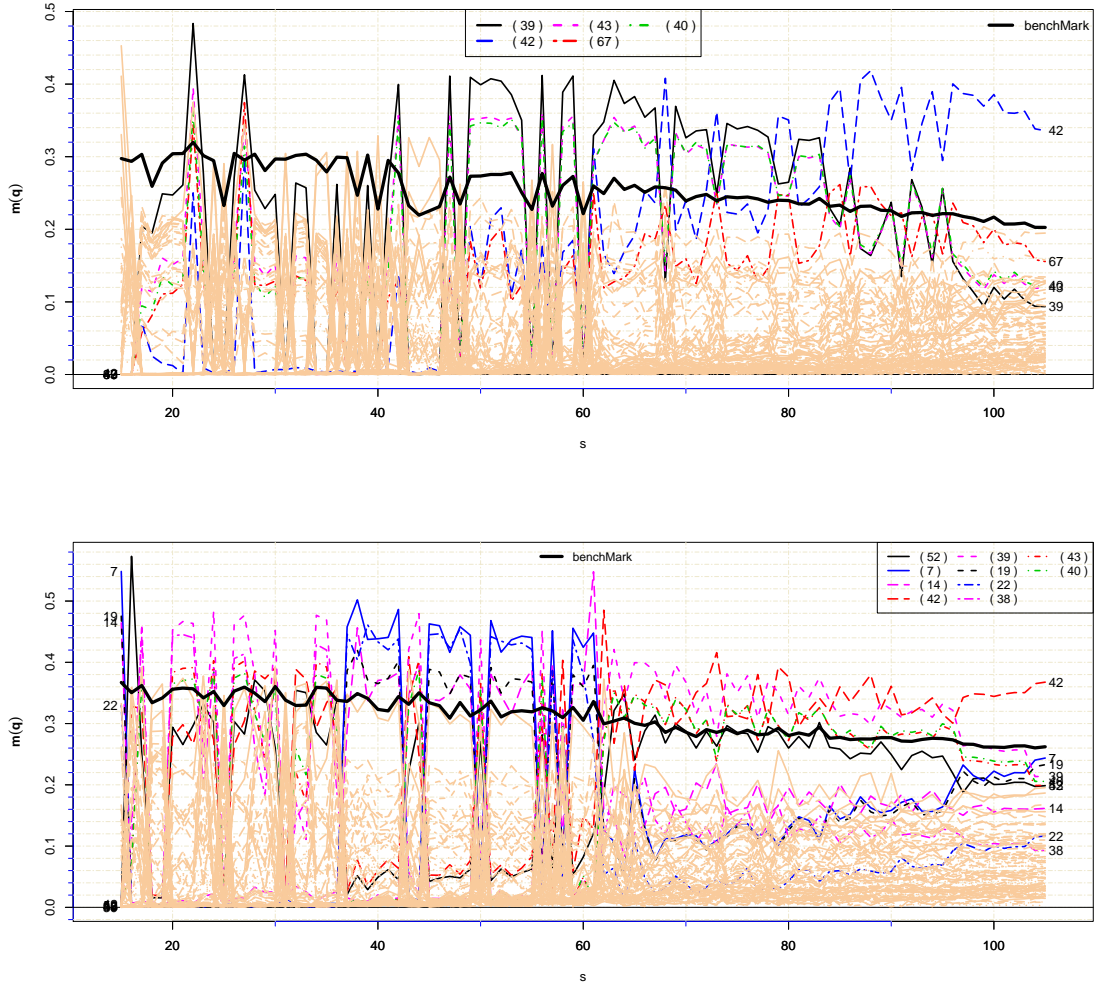
The first panel of Figure 7 (top) refers to the forward plot of CNCFS with  $q$  sufficiently large so that only the contribution of the largest eigenvalue and its associated eigenvector are considered, which clearly shows that only the observation 42 is above the benchmark in the last iteration. Therefore, the usual index plot of  $m(q)$  (Figure 8) would only give the conclusion that observation 42 might be influential.

Subject 42 had the highest pretest dental plaque index among individuals who used the experimental mouth rinse A and also it was already concluded that this observation is influential (see variance perturbation scheme). Although observation 42 is the one that appears in the last iteration with the whole data set as a possibly influential observation, observations (39,40,43) are above the benchmark in the middle to near the final part of the evolution of the forward search and they are masked in the final part. These observations also appeared as influential in variance perturbation scheme and response variable perturbation scheme. Moreover, these three observations have similar behavior during the evolution of the forward search. In addition, observation 67 stands out from the benchmark in some steps and has similar behavior as observation 42.

Table 1 shows that the hypothesis that the dental plaque index reduction after six months using the experimental mouth rinses A and B is the same is rejected at significance level 10%. On the other hand, if we drop the observations 42, 67 or (42,67) it is no longer rejected.

Table 2 shows that the hypothesis that the dental plaque index reduction of the adults who used the control mouth rinse and the experimental mouth rinse A after

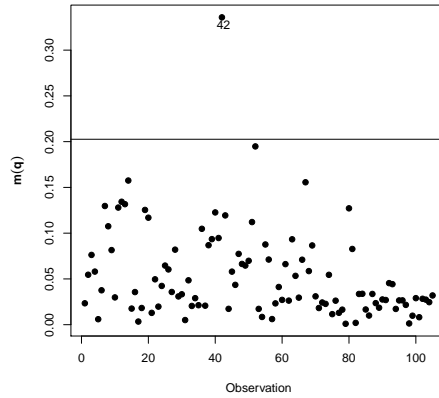
three months is the same is rejected. But, if we remove observations (39,40,43) it is no longer rejected at significance level of 1 %. An interesting point is that if we remove observations (39,40,43,42) the conclusion does not change compared to the conclusion with the whole data set.



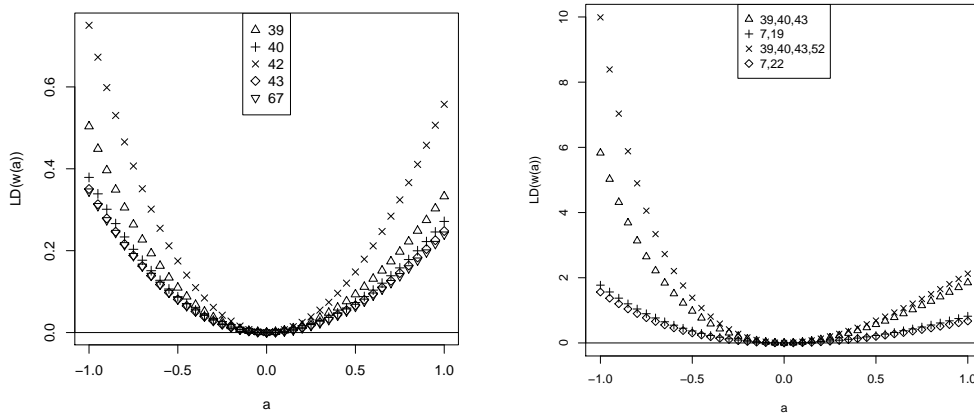
**Figure 7.** Mouth rinse data: CNCFS forward plots for case weight perturbation scheme. Contribution of the eigenvector associated with the largest eigenvalue (top) and aggregate contribution of the two largest eigenvalues and the associated eigenvectors (bottom).

Figure 9 (left hand panel) shows the plot of  $LD(\omega_0 + a\mathbf{l})$  versus  $a \in [-1, 1]$  along the directions  $\mathbf{l} = \mathbf{l}_k$ , with  $k = 39, 40, 42, 43$  and  $67$ . Observation 42 causes the greatest change in the likelihood displacement followed by observation 39. The influence of the observations 40, 43 and 67 are very close.

Considering the aggregate contribution of the two largest eigenvalues and the associated eigenvectors with the use of the case weight perturbation scheme (Figure 7, bottom), clearly only the observation 42 are above the benchmark in the final step of CNCFS which refers to the usual index plot of  $\mathbf{m}(q)$ .



**Figure 8.** Mouth rinse data: contribution of the eigenvector associated with the largest eigenvalue, case weight perturbation scheme.



**Figure 9.** Mouth rinse data: case weight perturbation scheme. Plot of  $LD(\omega(a))$  versus  $a$  with  $\omega(a) = \omega_o + al..$

As in this case there are more observations above the benchmark than the other forward plots of CNCFS that we have analyzed earlier, one way to have an overview of the influence of each of the observations in each iteration is the heatmap.

Figure 10 shows the heatmap relative to the bottom panel of Figure 7, it shows the degree of influence of each observation in each iteration. This graph shows all the observations in the  $y$  axis and in the  $x$  axis is the number of the iteration. The more influential is the observation in that iteration, darker is the color in the heatmap. Therefore it allows an overview of the influence of each observation. It is a different way to see which observation is more influential in each iteration of CNCFS .

Considering the bottom panel of Figure 7 (see also Figure 10), observations (39,40,43) are above the benchmark in most of the iterations from  $s = 62$  to  $s = 96$  and they are masked in the final iterations. Also they have similar behavior during the evolution of the forward search. Moreover, observation 52 are close to the benchmark and also has similar behavior as observations 39, 40 and 43.

Furthermore, these observations can change the result of the hypotheses testing of

interest. Table 1 concludes that with significance level 10 % the dental plaque index reduction rate after 6 months using the experimental mouth rinse A and B are not the same. But if we remove the observation 52 the conclusion is not the same anymore. Also Table 2 shows that the hypothesis that the dental plaque index reduction of the adults who used the control mouth rinse and the experimental mouth rinse A after three months are the same is rejected. However, if we remove the group of observations (39,40,43,52) it is no longer rejected at significance level 5 %.

In addition, the right-hand panel of Figure 9 shows that observations (39,40,43,52) are jointly the most influential one in the plot followed by the group of observations (39, 40, 43).

So, these are important observations that should be detected.

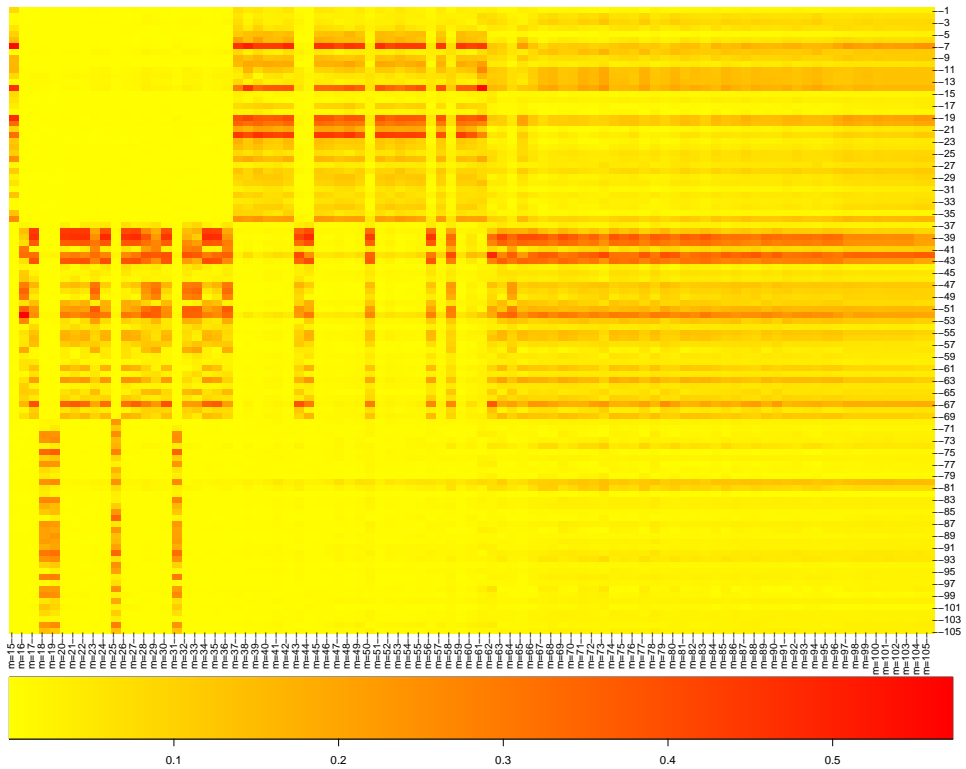


**Figure 10.** Mouth rinse data: case weight perturbation scheme - heatmap of the forward plot of CNCFS. Aggregate contribution of the two largest eigenvalues and the associated eigenvectors.

Considering the middle part of the evolution of the forward plot, observations (7,22) stands out, while observations (7,19) have similar behavior. These group of observations belong to the control mouth rinse treatment and they are the one that causes the least change in the likelihood displacement among the observations discussed earlier (right hand panel of Figure 9).

## 5. Hygroscopic Solid Dosage Data

### 5.1. Variance Perturbation Scheme

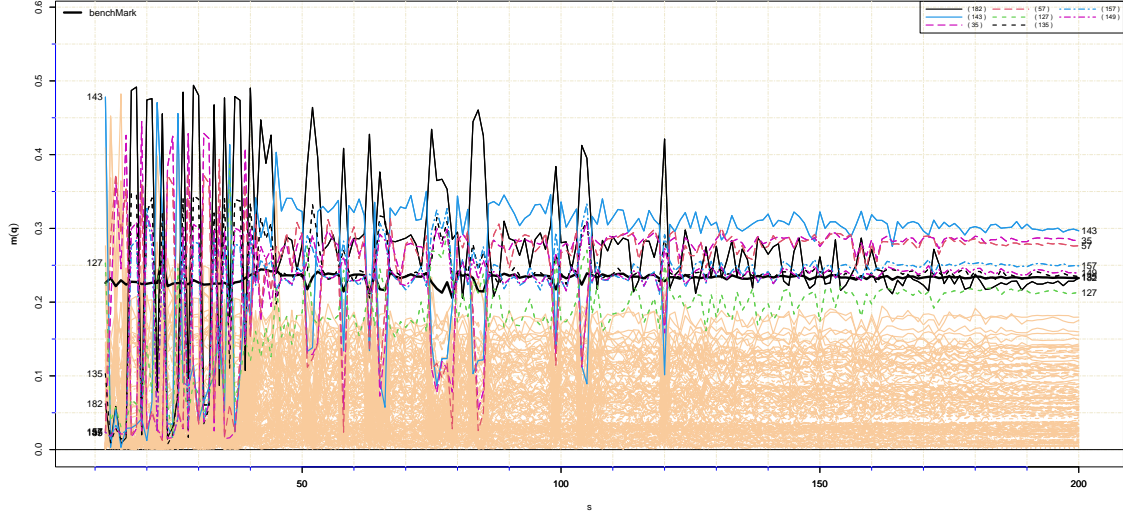


**Figure 11.** Hygroscopic solid dosage data: CNCFS forward plot for variance perturbation scheme. Aggregate contribution of the three largest eigenvalues and the associated eigenvectors.

Taking a look at the graph of Figure 11 (forward plot of CNCFS) observation 182 appears as a possibly influential observation in most of the iterations of CNCFS evolution. However, it is masked at iteration  $s = 181$  in the final part. Observation 182 is the solid dosage B with the highest moisture absorption from the beginning of the study until the end of the study among the solid dosages B and also the observation that absorbed the most moisture from the environment between the second and third follow-up time among the solid dosages B. Moreover, among observations that are above the benchmark in the final part of the evolution of CNCFS observations 143, 35 and 57 are detached from the rest of observations. Observation 143 is the observation with the highest moisture absorption from the beginning of the study up to 7 days from the beginning of the study among the solid dosage B. Observation 35 is the solid dosage A with the second highest weight at the beginning of the study and also after 7 days from the beginning of the study. It is also the observation with the least absorption from the second to third follow-up time among the solid dosages A. Observation 57 were commented before in the explanatory perturbation scheme.

Figure 12 shows the plot of  $LD(\omega_0 + a\mathbf{l})$  versus  $a \in [-1, 1]$  along the directions  $\mathbf{l} = \mathbf{l}_k$ , with  $k = 35, 57, 135, 143, 149, 157$  (observations that appears as possibly influential observations in the last iteration of CNCFS evolution or above the benchmark in the usual index plot of  $\mathbf{m}(q)$ ) and 182 (masked observation). In the negative side of  $a$  the masked observation, 182, is the most influential observation among the considered observations, while on the positive side of  $a$  it appears as the second most influential observation.

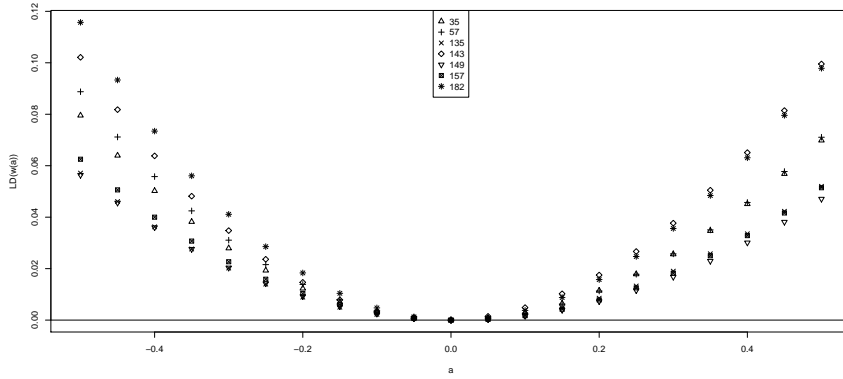


**Figure 12.** Hygroscopic solid dosage data: variance perturbation scheme. Plot of  $LD(\omega(a))$  versus  $a$  with  $\omega(a) = \omega_o + al$ .

### 5.2. Case Weight Perturbation Scheme

Considering the case weight perturbation scheme, it can be seen that observations 182 and 127 appears as possibly influential observations in most iterations in the first half of CNCFS evolution (Figure 13), but they are masked after iteration  $s = 139$ . Observation 182 appeared as masked observation in variance perturbation scheme and observation 127 also appeared as masked observation in explanatory variable perturbation scheme. Moreover, observation 6 are detached from the rest of observations that are above the benchmark in the final part of CNCFS evolution. Observation 6 is the solid dosage A with the least weight in the beginning of the study and also after 7 days among the solid dosages A. Also, it has the second least weight after 14 days.

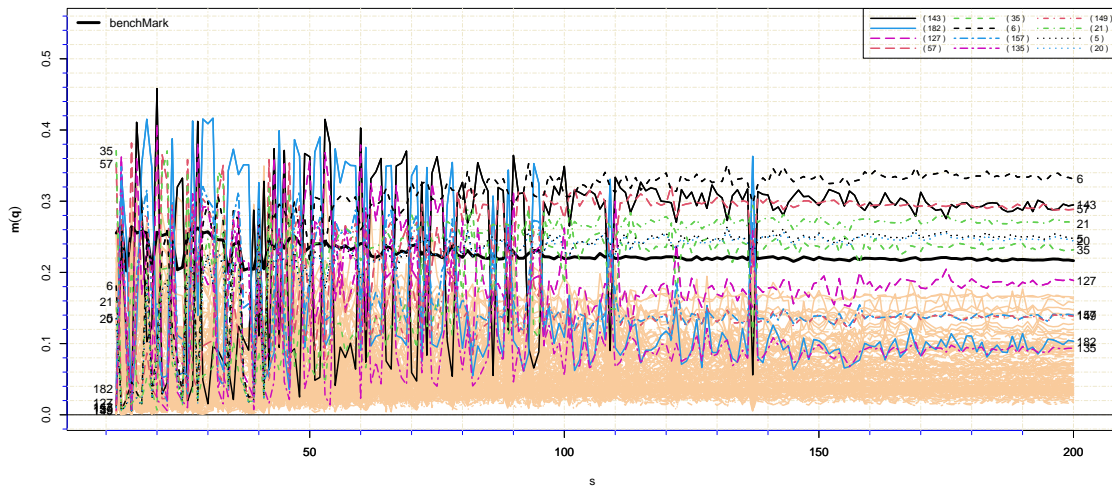


**Figure 13.** Hygroscopic solid dosage data: CNCFS forward plot for case weight perturbation scheme. Aggregate contribution of the three largest eigenvalues and the associated eigenvectors.

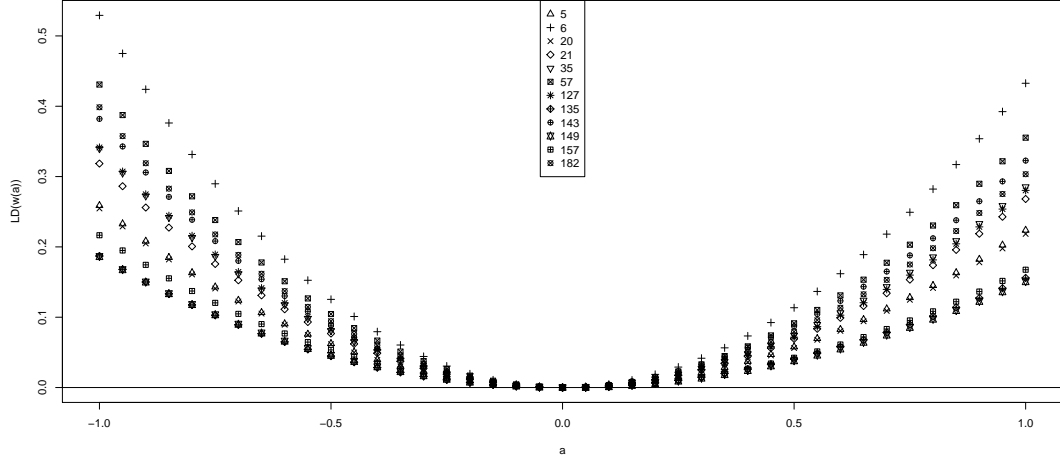


**Figure 14.** Hygroscopic solid dosage data: case weight perturbation scheme. Plot of  $LD(\omega(a))$  versus  $a$  with  $\omega(a) = \omega_o + al$ .

The plot of  $LD(\omega_0 + al)$  versus  $a \in [-1, 1]$  along the directions  $\mathbf{l} = \mathbf{l}_k$ , with  $k = 5, 6, 20, 21, 35, 57$  and  $143$  (observations that appears above the benchmark in the final part of the CNCFS evolution);  $127$  and  $182$  (masked observation commented above);  $149, 157$  and  $135$  (appears as possibly influential observations in the first half part of CNCFS evolution, but with less intensity than the observations  $127$  and  $182$ ) were obtained in Figure 14 to analyze the influence of these observations in the likelihood displacement. In the negative side of  $a$  observation  $6$  is the most influential, followed by observation  $57, 182$  (masked observation),  $143$  and  $127$  (masked observation). In the positive side of  $a$ , observation  $182$  appears as the forth most influential observation and observation  $127$  as the fifth most influential observation among the considered observations.